

Equilibrium Points and Zero Velocity Surfaces in the Restricted Four Body Problem with Solar Wind Drag

Reena Kumari

and

Badam Singh Kushvah

Department of Applied Mathematics,

Indian School of Mines, Dhanbad - 826004, Jharkhand, India

reena.ism@gmail.com; bskush@gmail.com

ABSTRACT

We have analyzed the motion of an infinitesimal mass in the restricted four body problem with solar wind drag. It is assumed that forces which govern the motion are mutual gravitational attractions of the primaries, radiation pressure force and solar wind drag. We have derived the equations of motion and find the Jacobi integral, zero velocity surfaces and particular solutions of the system. It is found that three collinear points are real when radiation factor $0 < \beta < 0.1$ whereas only one real point obtained when $0.125 < \beta < 0.2$. Again, stability property of the system is examined with the help of Poincaré surface of section (PSS) and Lyapunov characteristic exponents (LCEs). It is found that in presence of drag forces LCE is negative for a specific initial condition, hence the corresponding trajectory is regular whereas regular islands in the PSS are expanded.

Subject headings: Restricted four body Problem; radiation pressure; zero velocity surface; P-R drag; solar wind; PSS; LCE

1. Introduction

In space dynamics there are a number of systems like two body, three body, four body, N-body problem etc. The simplicity and elusiveness of the three body problem in different form like restricted three body problem (RTBP), restricted four body problem (RFBP) (may be consider as an approximation of two three body problem) etc. have attracted the attention of researchers for centuries. The motion of a spacecraft or satellite in the Sun-Earth-Moon system is a simple example of RFBP in space. The restricted four body has many possible uses in the dynamical system for example, the fourth body is very useful for saving fuel and time in the trajectory transfers in the restricted four body problem (Machuy et al 2007).

The description of the effect of radiation pressure force was first time given by Poynting (1903) and the effect of total radiation force on a par-

ticle P due to radiation source \mathbf{S} was analyzed by Robertson (1937) with the help of the general relativity theory. He stated that if we consider only first order term in $\frac{v}{c}$ then it consists a justifiable approximation in classical mechanics to yield (Ragos et al 1995)

$$F = F_p \left(\frac{\vec{r}}{r} - \frac{\vec{v} \cdot \vec{r}}{cr} \frac{\vec{r}}{r} - \frac{\vec{v}}{c} \right), \quad (1)$$

where $F_p = \frac{3LM}{16\pi R^2 \rho A c}$ denotes the measure of the radiation pressure force, \vec{r} is the position vector of P with respect to the Sun, \vec{v} is the corresponding velocity vector and c is the velocity of light. In expression of F_p , L is the luminosity of the radiating body whereas M , ρ and A are the mass, density and cross section of the particle respectively. In equation (1) on right hand side, first term expresses the radiation pressure and second term represents the Doppler shift owing to the motion of the particle whereas third term comes

on account of the absorption and subsequent re-emission of the radiation. The last two terms are called P-R drag effect.

Now, due to the solar wind drag force, equation (1) can be written as (Burns et al 1979)

$$m\ddot{\vec{r}} = \frac{SAQ_{pr}}{c} \left[\left(1 - (1 + sw) \frac{\vec{v} \cdot \vec{r}}{c r} \right) \frac{\vec{r}}{r} - (1 + sw) \frac{\vec{v}}{c} \right], \quad (2)$$

where S and Q_{pr} are the solar energy flux density and the radiation pressure coefficient respectively whereas sw represents the ratio of solar wind drag to Poynting-Robertson(P-R) drag (Liou et al 1995). The velocity independent term in (2) denotes the radiation pressure however velocity dependent term represents the drag force. The solar wind drag arises from the interaction between solar wind ions and the dust particles. The radiation pressure coefficient Q_{pr} depends on the properties of the particle P and the radiation factor β is defined by $\beta = \frac{\text{radiation pressure force}}{\text{solar gravitation force}} = \frac{SAQ_{pr}r_s^2}{cGMm}$.

Few years ago, Burns et al (1979) discussed about the radiation forces on small particles in the solar system and examined the different types of effect of the radiating body. However, Schuerman (1980) determined the equilibrium points and examined their stability in the presence of radiation pressure and P-R drag forces. The dynamical effect of general drag force (i.e. gas drag, nebular drag, PR drag etc.) in the planar circular restricted three body problem was described by Murray (1994). Also, he has examined the stability of Lagrangian equilibrium points using linear approximation. Further, Liou et al (1995) analyzed the effect of radiation pressure, P-R drag and solar wind drag on the motion of dust grains which is trapped in mean motion resonances with the Sun and the Jupiter in the restricted three body problem and found that all dust gains orbits are unstable. Again, Kalvouridis et al (2006) discussed the effect of radiation force due to primaries in the restricted four body problem using Radzievskii's model and noticed that there are some variations in the result which are unstable for all values of the parameters assumed by him. Further, Ishwar and Kushvah (2006) and Kushvah (2008), studied the restricted three body problem with P-R drag and examined the effect of P-R drag

force on the motion of infinitesimal body.

Lyapunov characteristic exponent (LCE) and Poincaré surfaces of section (PSS) are efficient method to study the behavior of orbit around the equilibrium points. The LCE are very useful tool for the estimation of chaoticity of the trajectory in a dynamical system. Basically, it measure the rate of exponential divergence between neighborhood trajectories in the phase space. The basic concepts of LCE was given by Oseledec (1968) during the study of ergodic theory of dynamical system. The description of numerical algorithm to calculate LCE was presented by Benettin et al (1980) and Froeschle (1984). Whereas the determination of the stability regions of the infinitesimal body was first time introduced by Poincaré (1892) during the study of periodic orbit of the system. This is a good technique to study the nature of trajectory of infinitesimal body and also known as surface of section method. Further, this method was used by Winter (2000) to describe the location and stability of orbit in the restricted three body problem.

A number of various type of four body models have been studied by many authors (Huang 1968; Hadjidemetriou 1980; Michalodimitrakis 1981; Rosaev 2011; Ceccaroni and Biggs 2012) etc. In these models, they have assumed either one or more bodies as radiating and minor body as very small in comparison to massive bodies. To preserve conservative character these models have been studied by ignoring dissipative forces like Poynting-Robertson(P-R) drag and solar wind drag. However, some of the research work in RFBP in addition with radiation pressure, P-R drag etc. have been performed by many authors (Kalvouridis et al 2006; Papadakis 2007; Machuy et al 2007; Medvedev and Perov 2008) etc. But, little attention has been paid on the effect of solar wind drag such models. Therefore, we have considered a restricted four body problem with radiation pressure and solar wind drag.

In order to know the nature of trajectory of infinitesimal body in the proposed problem, we have determined first order LCE for the maximal evolution time $0 \leq t \leq 10000$ with the help of algorithm given in Skokos (2010). The PSS of the proposed problem is also obtained with the help of Event Locator Method. We have used Mathematica[®] (Wolfram 2003) for numerical and algebraic com-

putation.

The formulation of the problem and derivation of equations of motion are presented in section (2) whereas in section (3), we have obtained the zero velocity surfaces with different cases and location of the collinear equilibrium points is computed in section (4). Section (4.4), we have discussed about the non-collinear equilibrium points however in section (5) we examine the stability behavior of the trajectory in the present dynamical system. Finally, we conclude the paper in section (6).

2. Formulation of the problem and equations of motion

We have considered a restricted four body problem in which $m_i, i = 1, 2, 3$ be the masses of three bodies such that $m_3 > m_1 > m_2$, and m be the mass of infinitesimal body. It is assumed that m_3 be a radiating body with solar wind drag which revolves around common center of mass of m_1 and m_2 . The governing forces of the motion of infinitesimal body are gravitational attractions of three massive bodies in addition with radiation pressure force, P-R drag and solar wind drag. It is also assumed that the effect of infinitesimal mass on the motion of the remaining system is negligible.

We use the canonical system of units, dividing all the distances by the distance between two primaries and dividing all the masses by the total mass of the two primaries. Under these assumption, the mean motion of primaries is taken as unity.

The masses and distances of the Earth, the Moon and the Sun are described as follows: mass of the Earth(M_E) = $5.98 \times 10^{24} kg$; mass of the Moon(M_M) = $7.35 \times 10^{22} kg$; mass of the Sun(M_S) = $1.99 \times 10^{30} kg$; distance between the Earth and the Moon is $d_1 = 3.844 \times 10^5 km$; distance between the Sun and the Earth is $d_2 = 1.496 \times 10^8 km$. Again, the masses of the Earth, the Moon and the Sun in the canonical system are given as $\mu_E = \frac{M_E}{M_M + M_E} = 0.987871$, $\mu_M = \frac{M_M}{M_M + M_E} = 0.012151$ and $\mu_S = \frac{M_S}{M_M + M_E} = 328900.48$ respectively.

Let μ_E and μ_M be the radii of the Moon and the Earth respectively and $(x, y), (x_E, y_E), (x_M, y_M)$ and (x_S, y_S) be the co-ordinates of the spacecraft, the Earth, the Moon and the Sun respectively (figure 1).

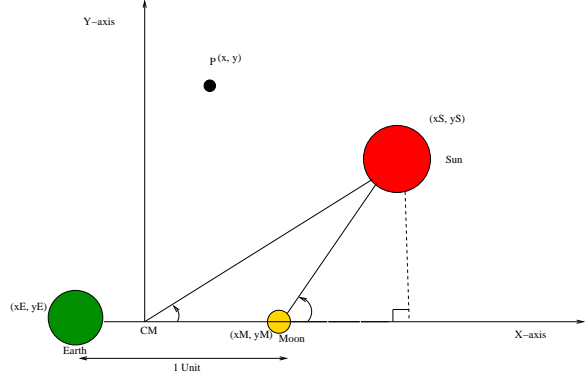


Fig. 1.— Geometry of the problem

Let $x_E = -\mu_M \cos(t), y_E = -\mu_M \sin(t), x_M = \mu_E \cos(t), y_M = \mu_E \sin(t), x_S = R_S \cos(\psi), y_S = R_S \sin(\psi)$ and $\psi = \psi_0 + \omega_s t$, where $R_S = 389.1724$ is the distance between the Sun and the center of mass of the system, $\omega_S = 0.07480$ is the angular velocity of the Sun which makes an angle ψ with x-axis, ψ_0 is the initial value of ψ and t is the time. The distances of spacecraft from the Earth, the Moon and the Sun are given as $r_1 = \sqrt{(x - x_E)^2 + (y - y_E)^2}$, $r_2 = \sqrt{(x - x_M)^2 + (y - y_M)^2}$ and $r_3 = \sqrt{(x - x_S)^2 + (y - y_S)^2}$ respectively.

The equations of motion of the infinitesimal mass in the inertial reference system are

$$\ddot{x} = -\frac{\mu_E(x - x_E)}{r_1^3} - \frac{\mu_M(x - x_M)}{r_2^3} - \frac{\mu_S(1 - \beta)(x - x_E)}{r_3^3} + (1 + sw)F_{PR,x}, \quad (3)$$

$$\ddot{y} = -\frac{\mu_E(y - y_E)}{r_1^3} - \frac{\mu_M(y - y_M)}{r_2^3} - \frac{\mu_S(1 - \beta)(y - y_E)}{r_3^3} + (1 + sw)F_{PR,y}, \quad (4)$$

where

$$F_{PR,x} = -\frac{\beta\mu_S}{cr_3^2} [k_1(x - x_S) + \dot{x}], \quad (5)$$

$$F_{PR,y} = -\frac{\beta\mu_S}{cr_3^2} [k_1(y - y_S) + \dot{y}]. \quad (6)$$

But,

$$k_1 = \frac{\{(x - x_S)\dot{x} + (y - y_S)\dot{y}\}}{r_3^2}$$

In the above expression $q_1 = (1 - \beta) = (1 - \frac{F_p}{F_g})$ and c are the mass reduction factor and dimensionless speed of the light respectively whereas F_p and F_g are the radiation pressure and the gravitational force respectively.

Using the coordinate transformation $x = \xi \cos t - \eta \sin t$; $y = \xi \sin t + \eta \cos t$, equations (3) and (4) become in the rotating reference frame as:

$$\ddot{\xi} - 2\dot{\eta} = \xi - \frac{\mu_E(\xi - \xi_E)}{r_1^3} - \frac{\mu_M(\xi - \xi_M)}{r_2^3} - \frac{\mu_S(1 - \beta)(\xi - \xi_S)}{r_3^3} + (1 + sw)F_{PR,\xi}, \quad (7)$$

$$\ddot{\eta} + 2\dot{\xi} = \eta - \frac{\mu_E(\eta - \eta_E)}{r_1^3} - \frac{\mu_M(\eta - \eta_M)}{r_2^3} - \frac{\mu_S(1 - \beta)(\eta - \eta_S)}{r_3^3} + (1 + sw)F_{PR,\eta}, \quad (8)$$

or

$$\ddot{\xi} - 2\dot{\eta} = \frac{\partial U}{\partial \xi} + (1 + sw)F_{PR,\xi}, \quad (9)$$

$$\ddot{\eta} + 2\dot{\xi} = \frac{\partial U}{\partial \eta} + (1 + sw)F_{PR,\eta}, \quad (10)$$

where

$$U = \frac{\mu_E}{r_1} + \frac{\mu_M}{r_2} + \frac{\mu_S(1 - \beta)}{r_3} + \frac{\xi^2 + \eta^2}{2}, \quad (11)$$

is the potential in the rotating coordinate system. The P-R drag components in (ξ, η) reference system are

$$F_{PR,\xi} = -\frac{\beta\mu_S}{cr_3^2} \left[\left\{ \dot{\xi} - (\eta - \eta_S) \right\} + n_1(\xi - \xi_S) \right]$$

and

$$F_{PR,\eta} = -\frac{\beta\mu_S}{cr_3^2} \left[\left\{ \dot{\eta} + (\xi - \xi_S) \right\} + n_1(\eta - \eta_S) \right],$$

where

$$n_1 = \frac{\left\{ (\xi - \xi_S)\dot{\xi} + (\eta - \eta_S)\dot{\eta} \right\}}{r_3^2}.$$

If we multiply the first equation (9) by $\dot{\xi}$ and the second equation (10) by $\dot{\eta}$ and adding, we get

$$\begin{aligned} \dot{\xi}\ddot{\xi} + \dot{\eta}\ddot{\eta} &= \frac{\partial U}{d\xi} \frac{d\xi}{dt} + \frac{\partial U}{d\eta} \frac{d\eta}{dt} + \\ (1 + sw) \left[\frac{\partial F}{d\xi} \frac{d\xi}{dt} + \frac{\partial F}{d\eta} \frac{d\eta}{dt} \right]. \end{aligned} \quad (12)$$

Since U and F do not depend explicitly on time, the expression on the right hand side is the total time derivative of U and F . The left hand side can be expressed in terms of the derivatives of the velocities:

$$\frac{1}{2} \frac{d}{dt} \left[\dot{\xi}^2 + \dot{\eta}^2 \right] = \frac{dU}{dt} + (1 + sw) \frac{dF}{dt}, \quad (13)$$

where

$$\begin{aligned} \frac{dF}{dt} &= -\frac{\beta\mu_S}{cr_3^2} \left[\frac{\left\{ (\xi - \xi_S)\dot{\xi} + (\eta - \eta_S)\dot{\eta} \right\}^2}{r_3^2} \right. \\ &\quad \left. - \left\{ (\eta - \eta_S)\dot{\xi} - (\xi - \xi_S)\dot{\eta} \right\} + \dot{\xi}^2 + \dot{\eta}^2 \right]. \end{aligned} \quad (14)$$

Integrating of equation (13) with respect to time, gives

$$\dot{\xi}^2 + \dot{\eta}^2 = 2U + 2(1 + sw)F - C$$

or

$$C = 2U + 2(1 + sw)F - v^2, \quad (15)$$

where v is the velocity of infinitesimal body and C is a constant, called the Jacobi integral. Now, the square of the velocity cannot be negative, the motion of the negligible body is restricted to the region where

$$v^2 = 2U + 2(1 + sw)F - C \geq 0$$

or

$$U + (1 + sw)F \geq \frac{C}{2}. \quad (16)$$

When the position and velocity of the negligible body are known for some initial moment, then we can obtain the Jacobi integral. Since U and F are functions of position and potential of dissipative force only, condition (16) tells immediately whether the system can ever reach a given point (ξ, η) . This condition does not tell about the shape

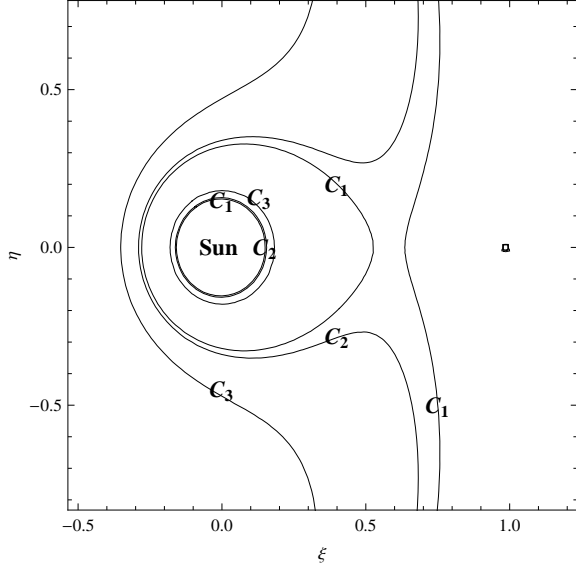


Fig. 2.— Zero velocity curves at $C_1 = 848.255$, $C_2 = 742.489$, $C_3 = 679.026$.

of the orbit, it only determines the region where the particle could move. Also, condition(16) shows that the larger value of C , the smaller the allowed region.

When C is large, the allowed region consists of the four separate areas. It can never moves from one allowed region to another if the regions are not connected. When C becomes smaller, a connection opens first at the point L_1 . Again, we take C even smaller, a connection opens between two inner regions, first at the point L_2 and second at the point L_3 . The small body can never escape from the system. Its orbit is then stable. Finally, when the value of C is further reduced, the outer and inner regions become connected and escape is possible which can be seen in the figure (2). It is also observe that how does the connection open with the decreases value of C . Figure(3) and (4) are the zoom portions of the regions around the Earth and the Moon. The points L_1, L_2, L_3 lie on the same straight line which connects the primaries.

When there are no dissipative forces i.e. $F_{PR,i} = 0$, then constant of the motion and the Jacobi constant C is defined as

$$C = 2U - (\dot{\xi}^2 + \dot{\eta}^2), \quad (17)$$

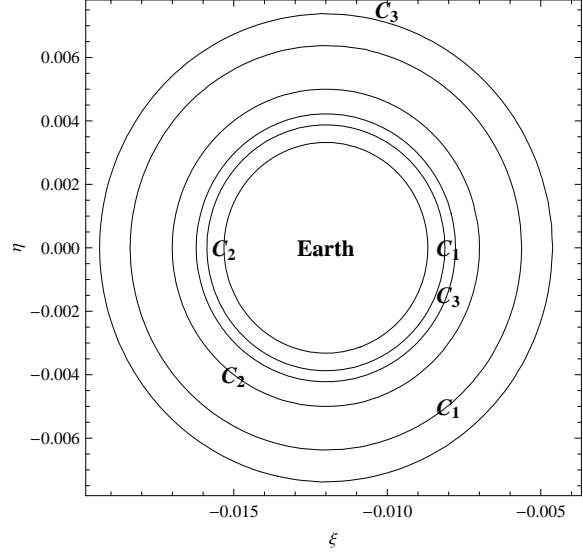


Fig. 3.— Zoom part of figure (2) at $\xi \in (-0.015, -0.005)$, $\eta \in (-0.006, 0.006)$, $C_1 = 848.255$, $C_2 = 742.489$, $C_3 = 679.026$.

which gives the results as in classical model of restricted three body problem. Again, equation (15) can be written as

$$C = 2U + b_1 + b_2 - \dot{\xi}^2 - \dot{\eta}^2, \quad (18)$$

where

$$b_1 = \frac{2\beta\mu_S(1+sw)}{c} \left\{ \frac{1}{2((\xi - 389.172)^2 + \eta^2)} + \arctan\left(\frac{\eta}{\xi - 389.172}\right) \right\} \quad \text{and}$$

$$b_2 = -\frac{2\beta\mu_S(1+sw)}{c} \int \frac{(\dot{\xi}^2 + \dot{\eta}^2)}{(\xi - 389.172)^2 + \eta^2} dt.$$

The third term of equation (18) depends on the time due to drag force. Therefore this integration term shows that Jacobi constant depends upon the time (Murray and Dermott 1999; Liou et al 1995).

Consequently, with the help of equation (17), we obtain the time derivative of Jacobi constant in presence of drag forces which is given as

$$\dot{C} = 2(1+sw)\frac{\beta\mu_S}{cr_3^2} \left\{ \dot{\xi}^2 + \dot{\eta}^2 + \frac{n_1^2}{r_3^2} - \left\{ (\eta - \eta_S)\dot{\xi} - (\xi - \xi_S)\dot{\eta} \right\} \right\} \quad (19)$$

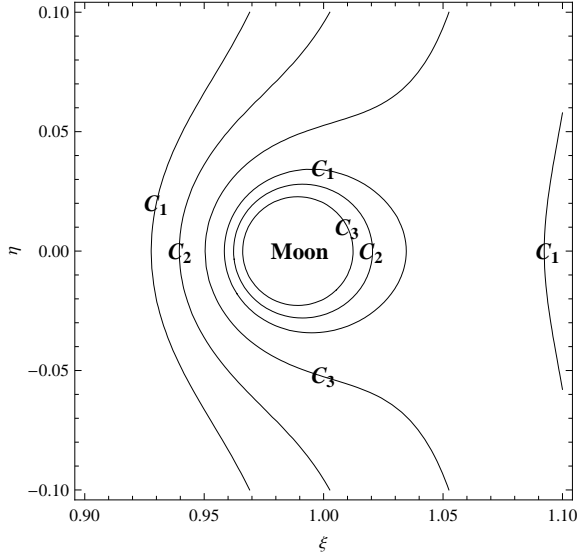


Fig. 4.— Zoom part of figure (2) at $\xi \in (0.9, 1.1)$, $\eta \in (-0.1, 0.1)$, $C_1 = 848.255$, $C_2 = 742.489$, $C_3 = 679.026$.

We have tried our best to derive the explicitly time independent expression of potential function or Jacobi constant but we could not find the exact analytical expression. In future, this should be taken up as a challenging problem of such models having P-R drag and solar wind drag.

3. Zero velocity surfaces

The Jacobi integral is a relation between the square of the velocity and the coordinates of the infinitesimal particle with respect to the set of rotating axes. If the particle's velocity becomes zero, we have

$$\xi^2 + \eta^2 + \frac{2\mu_E}{r_1} + \frac{2\mu_M}{r_2} + \frac{2(1-\beta)\mu_S}{r_3} + A_1 = C, \quad (20)$$

where

$$A_1 = \frac{2(1+sw)\beta\mu_S}{c} \left[\arctan\left(\frac{\xi - \xi_S}{\eta - \eta_S}\right) - \arctan\left(\frac{\eta - \eta_S}{\xi - \xi_S}\right) \right] \quad (21)$$

and C can be determined from the initial conditions.

Equation (20) is important in this problem and it is defined for a given value of C i.e. the bound-

aries of regions in which the particle is free to move. Now, for large values of ξ and η , all the terms except first and second in L.H.S. of the equation (20) become unimportant. In other words, this equation takes the form:

$$\xi^2 + \eta^2 = C - \sigma = C_1, \quad (22)$$

where

$$\sigma = \frac{2\mu_E}{r_1} + \frac{2\mu_M}{r_2} + \frac{2(1-\beta)\mu_S}{r_3} + A_1.$$

The equation (22) represents a circle whose radius is $\sqrt{C_1}$. Therefore the curve in the $\xi\eta$ - plane is an approximately oval shape within the asymptotic cylinder. For small values of ξ and η , the first and second terms are relatively unimportant, hence the equation may be written as:

$$\frac{\mu_E}{r_1} + \frac{\mu_M}{r_2} + \frac{(1-\beta)\mu_S}{r_3} + A_1 = C_2,$$

where

$$C_2 = \frac{1}{2} (C - \xi^2 - \eta^2), \quad (23)$$

which is an equation of equipotential surfaces.

Figure (5), shows that curves intersect at a point where function gives local minimum and maximum value of Jacobi constant. Again, figure (6) shows contour curves which are the equipotential boundaries. It is clear from the frames that the configuration rotates anti-clock wise with an angle ψ . In the contour plots red (dark) portion shows the higher equipotential value whereas when we go from red portion to blue (very dark) one, equipotential decreases gradually. Now, the zero velocity curves are defined by the equation

$$f(\xi, \eta) = \xi^2 + \eta^2 + \frac{2\mu_E}{r_1} + \frac{2\mu_M}{r_2} + \frac{2(1-\beta)\mu_S}{r_3} + A_1. \quad (24)$$

To determine the curvature of a zero velocity curve (ZVC) (24), we use the formula (Marčeta 2012)

$$ZVC = \frac{f_{\xi\xi}f_{\eta\eta}^2 - 2f_{\eta\xi}f_{\xi\xi}f_{\eta\xi} + f_{\eta\xi}f_{\xi\xi}^2}{(f_{\xi\xi}^2 + f_{\eta\eta}^2)^{3/2}}, \quad (25)$$

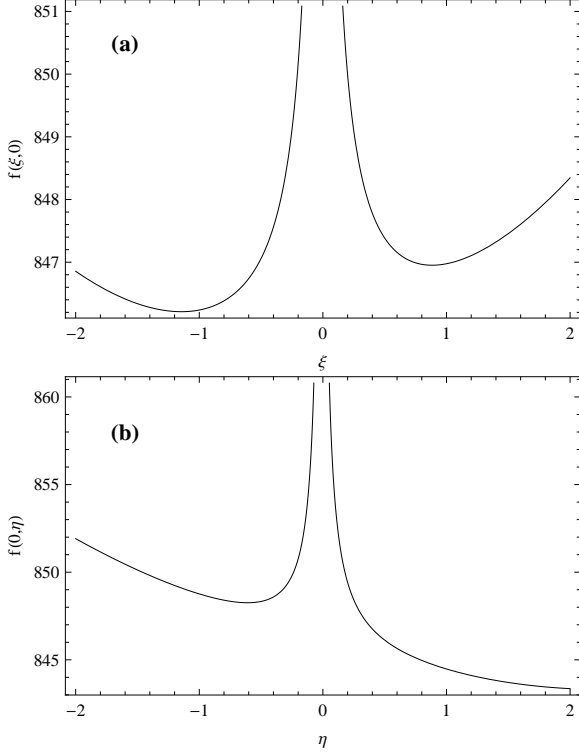


Fig. 5.— (a) $f(\xi, 0)$ and (b) $f(0, \eta)$ for $\mu_E = 0.987$, $\mu_M = 0.012$, $\mu_S = 328900.48$, $t = 1000$, $\psi = 0$, $\beta = 0.00002$, $c = 1.8 \times 10^6$, $sw = 0.248$.

where

$$f_\xi = \frac{\partial f(\xi, \eta)}{\partial \xi}, f_\eta = \frac{\partial f(\xi, \eta)}{\partial \eta}, f_{\xi\xi} = \frac{\partial^2 f(\xi, \eta)}{\partial \xi^2},$$

$$f_{\eta\eta} = \frac{\partial^2 f(\xi, \eta)}{\partial \eta^2}, f_{\xi\eta} = \frac{\partial^2 f(\xi, \eta)}{\partial \xi \partial \eta}.$$

Now, we determine the curvature of ZVC (24) with the help of characteristic values of Hessian matrix H , i.e.

$$H = \begin{bmatrix} \frac{\partial N_\xi}{\partial \xi} & \frac{\partial N_\xi}{\partial \eta} \\ \frac{\partial N_\eta}{\partial \xi} & \frac{\partial N_\eta}{\partial \eta} \end{bmatrix}, \quad (26)$$

where N_ξ and N_η are components of normal unit

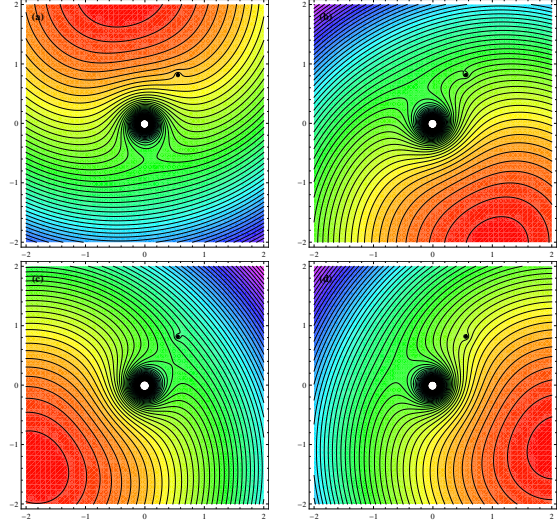


Fig. 6.— Zero velocity surfaces at (a) $\psi = 0$, (b) $\psi = 60$, (c) $\psi = 90$ and (d) $\psi = 180$.

vector defined by

$$\vec{N} = \begin{bmatrix} \vec{N}_\xi & \vec{N}_\eta \end{bmatrix} = \frac{\vec{G}}{\|\vec{G}\|}$$

$$= \frac{\begin{bmatrix} \frac{\partial f}{\partial \xi} & \frac{\partial f}{\partial \eta} \end{bmatrix}}{\left[\left(\frac{\partial f}{\partial \xi} \right)^2 + \left(\frac{\partial f}{\partial \eta} \right)^2 \right]^{1/2}}, \quad (27)$$

with

$$\vec{G} = \nabla f = \begin{bmatrix} \frac{\partial f}{\partial \xi} & \frac{\partial f}{\partial \eta} \end{bmatrix}. \quad (28)$$

Since the expression of the curvature of zero velocity curve is too complicated to deduce anything meaningful analytically. Therefore we have computed curvatures numerically and observe that the curvature of any curve shows the bending nature at a particular point (figures 7, 8 and 9). This value is inverse proportional to the radius of curvature. If curvature is large then radius of curvature is small, that means curve is more bended at that point. If curvature decreases then radius of curvature increases, that means bending property of the curve decreases which opens the path to move particle freely. From figure(9) it can be seen that around the singular points, curvature of zero velocity curve is highest that means radius of curvature is least therefore curves are disjoint closed loops form where particles can move form

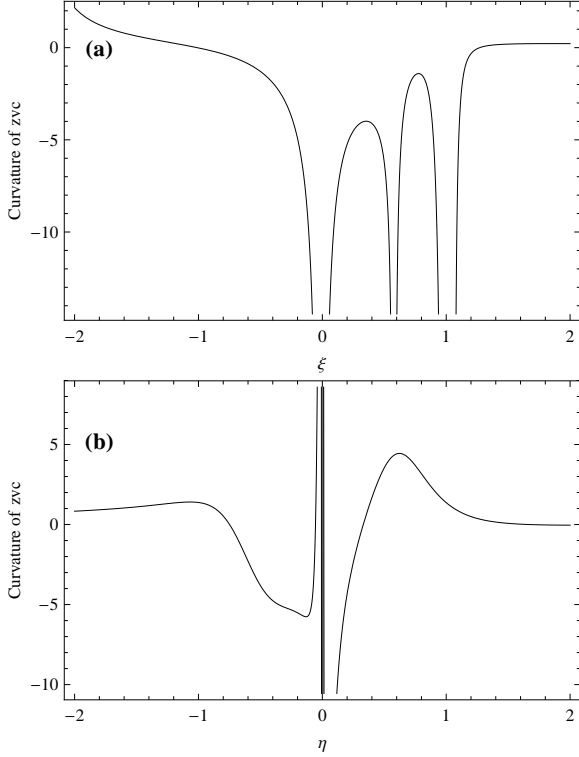


Fig. 7.— Curvature of (a) $f(\xi, 0)$ and (b) $f(0, \eta)$ for $\mu_E = 0.987$, $\mu_M = 0.012$, $\mu_S = 328900.48$, $t = 0$, $\psi = 0$, $\beta = 0.00002$, $c = 1.8 \times 10^6$, $sw = 0.248$.

one regions to another. In figure (7), frames (a) and (b) show the curvature of ZVC depends on ξ and η respectively and indicates that the curves are sometimes nearer to each other and sometimes goes far from each other. When the curves bend to each other then the connection opens where the body moves from one allowed side to another side. When the curve is not bended that means curve goes outside, then the curves are separate (figure 8). Different layers show the equipotential curvatures where the movement is possible which is clearly seen in zoom part of the figure (8). Also, figure (9) shows the curvature of zero velocity surfaces, cut off portions indicate the singularities of the surfaces where motion of infinitesimal body is impossible.

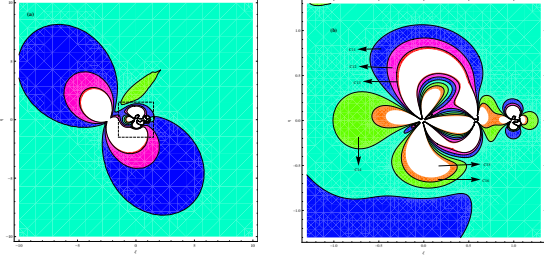


Fig. 8.— (a) Curvature of zero velocity surface and (b) Zoom of square portion of figure (a).

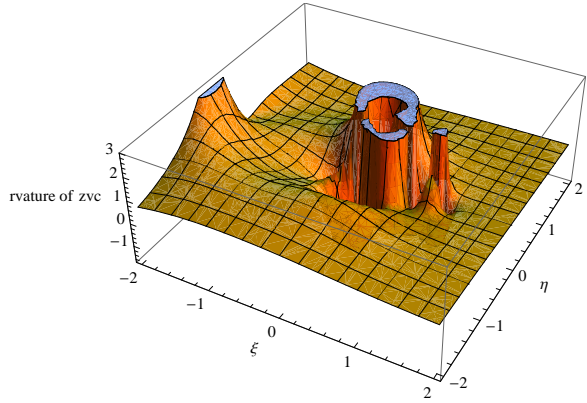


Fig. 9.— Curvature of zero velocity surfaces.

4. Location of the Lagrangian equilibrium points

For equilibrium points, we solve the equations (9) and (10) by taking $\dot{\xi} = 0 = \dot{\eta} = \ddot{\xi} = \ddot{\eta}$ i.e.

$$\xi - \frac{\mu_E(\xi - \xi_E)}{r_1^3} - \frac{\mu_M(\xi - \xi_M)}{r_2^3} - \frac{\mu_S(1 - \beta)(\xi - \xi_S)}{r_3^3} + (1 + sw)F_{PR,\xi} = 0, \quad (29)$$

$$\eta - \frac{\mu_E(\eta - \eta_E)}{r_1^3} - \frac{\mu_M(\eta - \eta_M)}{r_2^3} - \frac{\mu_S(1 - \beta)(\eta - \eta_S)}{r_3^3} + (1 + sw)F_{PR,\eta} = 0, \quad (30)$$

where

$$F_{PR,\xi} = \frac{\beta\mu_S}{cr_3^2}(\eta - \eta_S), \quad F_{PR,\eta} = -\frac{\beta\mu_S}{cr_3^2}(\xi - \xi_S).$$

4.1. Particular cases

1. When $\beta = 0$ then the equation (29) and (30) give the following

$$\xi - \frac{\mu_E(\xi - \xi_E)}{r_1^3} - \frac{\mu_M(\xi - \xi_M)}{r_2^3} - \frac{\mu_S(\xi - \xi_S)}{r_3^3} = 0,$$

$$\eta - \frac{\mu_E(\eta - \eta_E)}{r_1^3} - \frac{\mu_M(\eta - \eta_M)}{r_2^3} - \frac{\mu_S(\eta - \eta_S)}{r_3^3} = 0. \quad (31)$$

This is the classical case of restricted four body problem.

2. If $\beta = 1$ then the equation (29) and (30) takes the form

$$\xi - \frac{\mu_E(\xi - \xi_E)}{r_1^3} - \frac{\mu_M(\xi - \xi_M)}{r_2^3} + (1 + sw)F_{PR,\xi} = 0,$$

$$\eta - \frac{\mu_E(\eta - \eta_E)}{r_1^3} - \frac{\mu_M(\eta - \eta_M)}{r_2^3} + (1 + sw)F_{PR,\eta} = 0. \quad (32)$$

This becomes the restricted three body problem with solar wind and P-R drag.

4.2. Collinear points

The collinear points are solutions of the equations (29-30) with $\eta = 0$. That is, the collinear points lie on the line joining the primaries. Therefore, we have

$$\xi - \frac{\mu_E(\xi - \xi_E)}{r_1^3} - \frac{\mu_M(\xi - \xi_M)}{r_2^3} - \frac{\mu_S(\xi - \xi_S)}{r_3^3} = 0. \quad (33)$$

When the value of β is zero, the above equation becomes

$$\xi^7 - 780.294\xi^6 + 152974\xi^5 - 624960\xi^4 + 782507\xi^3 - 454193\xi^2 + 288215\xi - 145671 = 0, \quad (34)$$

which shows that the roots lie in the ξ axis and after simplification, the above equation consists seven degree. Using the Descartes' rule of sign we found that three roots are real and other pair of roots are imaginary, because the coefficients of the power of ξ change seven signs. This shows that at a time we can have only three real roots joining the two primaries because the plane of motion of the Earth around the Sun is different from the plane of motion of the Moon around the Earth. The three primaries will be in the same plane when the Moon comes at the line of node of the plane of motion.

Now, if we take β non-zero then we obtain three real roots of equation (33) change with the value of $\beta \in (0, 0.1)$. Again, if $\beta \in (0.125, 0.2)$ then we have only one root which increases with β . With the help of these values we determine Jacobi constant and see that an increases in the value of β consequently the Jacobi constant decreases and the corresponding energy increases (Table 1).

4.3. Extremal values

From equation (20), we have

$$C = \xi^2 + \eta^2 + \frac{2\mu_E}{r_1} + \frac{2\mu_M}{r_2} + \frac{2(1 - \beta)\mu_S}{r_3} + \frac{2(1 + sw)\beta\mu_S}{c} \left[\int \frac{(\eta - \eta_S)}{r_3^2} d\xi - \int \frac{(\xi - \xi_S)}{r_3^2} d\eta \right] \quad (35)$$

$$\mu_E r_1^2 + \mu_M r_2^2 = \mu_E [(\xi - \xi_E)^2 + (\eta - \eta_E)^2] + \mu_M [(\xi - \xi_M)^2 + (\eta - \eta_M)^2],$$

$$\Rightarrow \mu_E r_1^2 + \mu_M r_2^2 = \xi^2 + \eta^2 + \mu_E \mu_M,$$

$$\Rightarrow \xi^2 + \eta^2 = \mu_E r_1^2 + \mu_M r_2^2 - \mu_E \mu_M.$$

Substituting these values in equation (35), we get

$$\phi = \mu_E \left[r_1^2 + \frac{2}{r_1} \right] + \mu_M \left[r_2^2 + \frac{2}{r_2} \right] + \frac{2(1 + sw)\beta\mu_S}{c} \left[\frac{\int (\eta - \eta_S) d\xi}{r_3^2} - \frac{\int (\xi - \xi_S) d\eta}{r_3^2} \right] - \mu_E \mu_M + \frac{2(1 - \beta)\mu_S}{r_3}. \quad (36)$$

Differentiating equation (36) with respect to r_1, r_2 and r_3 respectively and equating each term to zero

Table 1: Collinear points for initial parameters $\mu_E = 0.987$, $\mu_M = 0.012$, $\mu_S = 328900.48$, $t = 0$, $\psi = 0$

β	I	II	III	C_1	C_2	C_3
0.0	-1.86495	-0.892772	0.578692	843.374	844.720	848.255
0.0000025	-1.86494	-0.892775	0.578693	843.372	844.718	848.253
0.000005	-1.86494	-0.892778	0.578693	843.370	844.716	848.251
0.0000075	-1.86493	-0.892780	0.578694	843.368	844.714	848.249
0.00001	-1.86492	-0.892783	0.578694	843.366	844.712	848.247
0.0000125	-1.86491	-0.892786	0.578695	843.364	844.709	848.245
0.0000150	-1.86490	-0.892789	0.578695	843.362	844.707	848.242
0.0000175	-1.86490	-0.892792	0.578696	843.359	844.705	848.240
0.00002	-1.86489	-0.892795	0.578696	843.357	844.703	848.238
0.025	-1.78593	-0.924049	0.583721	822.399	823.571	827.103
0.05	-1.70064	-0.961693	0.588858	801.429	802.416	805.950
0.075	-1.60522	-1.009590	0.594104	780.467	781.248	784.796
0.10	-1.48925	-1.078140	0.599462	759.527	760.056	763.643
0.125	Complex	Complex	0.604934	Complex	Complex	742.489
0.150	Complex	Complex	0.610524	Complex	Complex	721.335
0.175	Complex	Complex	0.616232	Complex	Complex	700.181
0.20	Complex	Complex	0.622061	Complex	Complex	679.026

for initial values of t , we get

$$r_1 = 1, r_2 = 1, \\ r_3 = \frac{\beta}{\beta - 1} \frac{2 \times (1 + sw) \times R_s \times \eta}{c}. \quad (37)$$

In equation (37), if we take $r_3 = 0$, this causes the Sun to be placed at the origin which is not possible in the proposed system. Because for a moment if we consider that the Sun is placed at the common center of the Earth and the Moon and consequently, we get a system in which the Earth and the Moon revolve in different orbits about the Sun. In general such type of system does not exist for the problem in hand. If $r_3 > 0$ then the factor $\frac{(1+sw)\beta}{(\beta-1)} > 0$ has the following cases:

1. If $\frac{\beta}{(\beta-1)}(1 + sw)$ have positive signs then $sw > -1$ and β lies in the open interval $(0, 1)$ that is $\frac{F_p}{F_g} < 1$.

2. If $\frac{\beta}{(\beta-1)}$ and $(1 + sw)$ have negative signs then $sw < -1$ and β lies outside the open interval $(0,1)$ and the body escapes from the system.

The function ϕ always positive for any $r_i, i = 1, 2, 3$ and ϕ approaches to infinity as r_i approaches to zero or infinity. Therefore, the equilibrium points of the system are absolute minimum however the pseudo-potential and the Jacobi constant at these points are:

$$\phi = \frac{1}{(1 + sw) \beta \eta} A_2, \quad (38)$$

$$C = \frac{2}{(1 + sw) \beta \eta} A_2, \quad (39)$$

where

$$A_2 = -7.60616 \times 10^8 + \beta \eta \{1.52123 \times 10^9 \\ + (2.98516 + 2.98516 \times sw)\}. \quad (40)$$

4.4. Non-collinear points

For non-collinear points, we take perturbation in distances of infinitesimal mass from the primaries due to the radiation pressure and solar wind drag and suppose $r_1 = 1 + \epsilon_1$ and $r_2 = 1 + \epsilon_2$, where $\epsilon_1, \epsilon_2 \ll 1$, then from center of mass property, we obtain

$$\mu_E r_1 + \mu_M r_2 = 0 \Rightarrow \mu_E \epsilon_1 + \mu_M \epsilon_2 + 1 = 0. \quad (41)$$

Now, $r_1^2 - r_2^2 = (\xi + \mu_M)^2 + \eta^2 - (\xi + \mu_M - 1)^2 - \eta^2$, therefore

$$\xi = \frac{2(\epsilon_1 - \epsilon_2) + 1}{2} - \mu_M. \quad (42)$$

Substituting this value in the equation (29), we get

$$\eta = \pm \sqrt{\frac{-(1 - 3sw - 4\beta) \times c^2 \times (\xi - 389.172)}{2 \times (1 - sw - 2\beta) \times 389.172 \times \beta^2}}. \quad (43)$$

Again, substituting the value of ξ in the equation (29) and neglecting second and higher order terms of β , we get

$$\mu_S(1 - 4\beta)(1 - 3sw)c^3 \left(\frac{2(\epsilon_1 - \epsilon_2) + 1}{2} - \mu_M - 389.172 \right) = 0. \quad (44)$$

Solving equation (41) and (44), we get the values of ϵ_1 and ϵ_2 which are given below

$$\epsilon_1 = \frac{1}{-1 + 3sw + 4\beta} A_3, \\ \epsilon_2 = \frac{1}{-1 + 3sw + 4\beta} A_4, \quad (45)$$

where

$$A_3 = -12(0.0833 - 0.3333\beta - 0.25sw) \times \\ (0.0026 + \mu_M) \times (388.669 + \mu_M) \quad (46)$$

and

$$A_4 = 1 - 3sw - 4\beta + (4664.06 + 12\mu_M) \times \\ \mu_E(0.0833 - 0.3333\beta - 0.25sw). \quad (47)$$

Substituting the values of ϵ_1 and ϵ_2 in equation (42) and (43), we get the non-collinear points. These points depend on the values of the radiation pressure and the solar wind drag. When we change the values of ratio of solar wind to P-R drag parameter for different fixed values of radiation pressure parameter, points are changes. Numerically the coordinates of triangular equilibrium points are $L_4 f = (0.615824, 0.75845)$, $L_5 f = (0.615824, -0.75845)$ which are obtained by taking the same parametric values as earlier taken in

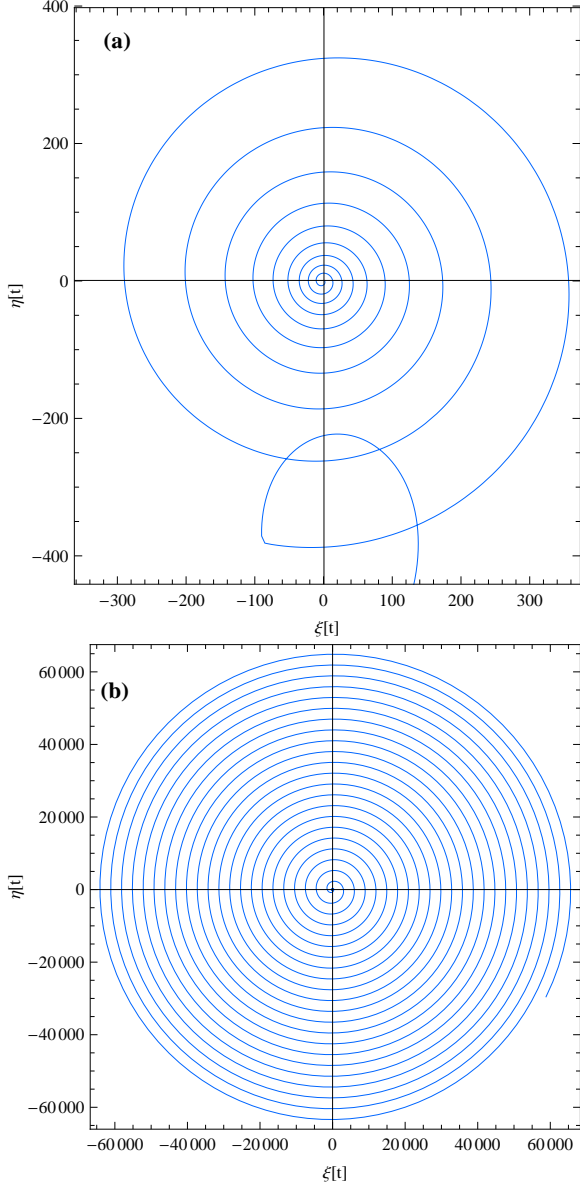


Fig. 10.— Trajectory of non-collinear points

case of collinear equilibrium points. The parametric solution (i.e. triangular point) is depicted in figure (10). Frame (a) of this figure shows that triangular point exists regularly for $0 \leq t \leq 60$ and then a sudden change in trajectory has been seen for $60 \leq t \leq 80$. Finally, solution maintains its regular path for $t > 80$. Whereas frame (b) of this figure shows the nature of the path of infinitesimal body for the time interval $0 \leq t \leq 200$. It is also found that the infinitesimal mass escapes out side of possible region after $t > 424229$.

5. Poincaré surfaces of section and Lyapunov characteristic exponents

The Poincaré surfaces of section (PSS) is an important technique to describe the stability region of the system. In order to determine the orbital element of the infinitesimal body at any instant, it is necessary to know its position (ξ, η) and velocity $(\dot{\xi}, \dot{\eta})$ correspond to a four dimensional phase space. In this paper, we have determined PSS in the $\xi\dot{\xi}$ -plane using Event Locator Method of Mathematica[®] (Wolfram 2003). The magnitude of the velocity component $\dot{\eta}$ is computed with the help of Jacobi integral equation (15) however the Jacobi constant C initially computed at $t = 0$. Now, we have plotted the graph of ξ and $\dot{\xi}$ against each other when the trajectory intersects the plane in the direction of $\dot{\eta} > 0$. In other words, a smooth well defined island in the PSS indicates that the trajectory is likely to be regular whereas the fuzzy distribution of intersection points represents chaotic trajectory. Again, if the curve shrink to a point that means it has a periodic orbit. Further, we have obtained PSS at the values of Jacobi constant C for a certain range of values of ξ and $\dot{\xi}$ whereas each orbit is determined with initial conditions:

$$\begin{aligned} \xi &= \xi_0, \quad \eta = 0, \quad \dot{\xi} = 0, \\ \dot{\eta} &= \sqrt{b_3 + b_4 + \xi_0^2 - \dot{\xi}_0^2 - C}, \end{aligned} \quad (48)$$

where

$$\begin{aligned} b_3 &= \frac{2\mu_E}{(\xi_0 + 0.012)} + \frac{2\mu_M}{(\xi_0 - 0.987)} + \frac{2\mu_S(1 - \beta)}{(\xi_0 - 389.172)} \\ \text{and} \\ b_4 &= \frac{2\beta\mu_S(1 + sw)}{c} \left\{ \frac{1}{2(\xi_0 - 389.172)^2} \right. \\ &\quad \left. + \arctan\left(\frac{\eta}{\xi_0 - 389.172}\right) \right\}. \end{aligned}$$

Since, in the proposed model key quantities are the values of C, β and sw . Therefore, we have plotted the graphs at these parameters. Figure (11) shows

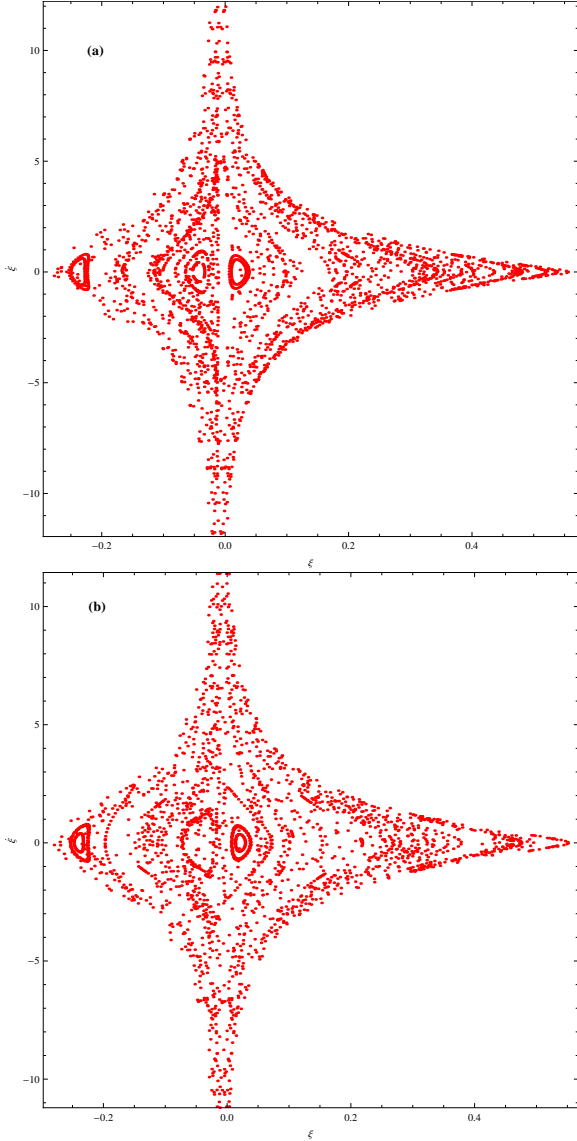


Fig. 11.— Poincare surfaces of section.

PSS for the restricted four body problem at the minimum values of Jacobi constant $C = 1696.48$ which is initially determined at $\xi = 0.5, \eta = 0, \dot{\xi} = 0, \dot{\eta} = 0$. In this figure, we observe that the nature of PSS and the trajectory in $\xi\eta$ -plane. From frame (a), we have seen regular island with the radiation pressure and the solar wind drag but frame (b) shows the regular island without any force. Here,

it is clear that the regular island expands gradually due to the effect of radiation pressure and solar wind drag. Again, the island at $\xi = 0.025$ shows that the trajectory is regular i.e. region in the neighborhood of $\xi = 0.025$ is stable. On the other hand, in frame (b) the island at 0.025 shows that the trajectory is regular and this region shrinks towards center. Hence from frames (a) and (b), we conclude that the radiation pressure and solar wind drag have significantly affect on the stability region of the trajectories.

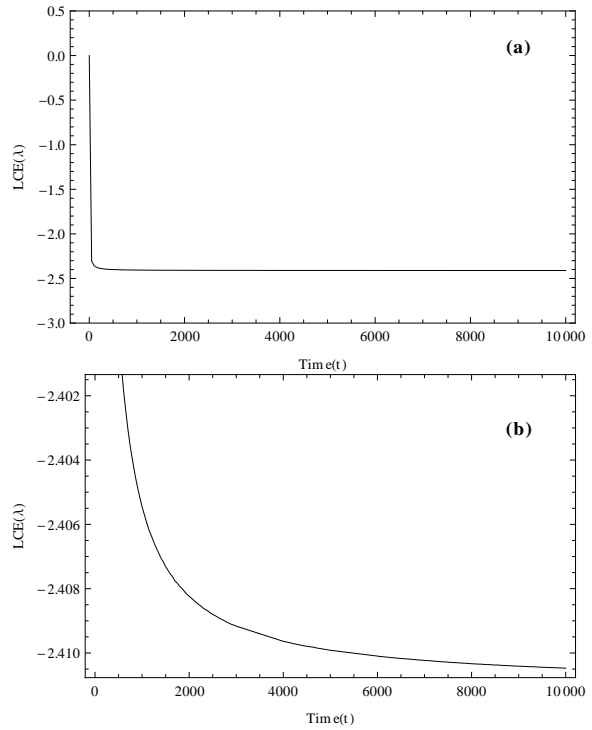


Fig. 12.— Lyapunov characteristic exponent: (a) for $0 \leq t \leq 10000$ (b) Zoom of (a).

In order to know the behavior of nearby trajectory emanating from the neighborhood of an equilibrium point we compute the LCEs. With the help of method and algorithm described in Skokos (2010), we have numerically computed first order LCEs and plotted the graphs t Vs $LCE(\lambda)$, upto maximum evolution of time $0 \leq t \leq 10000$ when $\mu_E = 0.987, \mu_M = 0.012, \mu_S = 328900.48, \beta = 0.00002, sw = 0.248, c = 1.8 \times 10^6$ (figure 12). This figure shows that the proposed model is slightly affected in presence of the radiation pressure and the solar wind drag. Also, it is clear that λ decreases

slowly with time. Furthermore, λ is negative for $0 \leq t \leq 10000$ which shows that orbit is regular in this interval. Therefore, we observed that the values of LCE depends on initial deviation vector and renormalized time step. As we have used default method of Mathematica[®] software package for the numerical solutions of the differential equations. The obtained result depends on precision and accuracy goals, i.e. in present problem, if these goals were chosen different from 3 consequently there was overflow in the result which leads to the false estimation of the LCE.

6. Discussion and conclusion

We have studied the restricted four body problem by assuming the effect of radiation pressure and solar wind drag. The boundaries of allowed regions for the motions of the infinitesimal mass are determined using zero velocity surfaces at different values of radiation pressure and solar wind drag. It is found that allowed possible regions of the motions decrease with the an increase in the value of Jacobi constant C . We have observed that in presence of drag forces, Jacobi constant depends on the time (Murray 1994; Liou et al 1995). The range of radiation pressure and solar wind drag are determined and found that motion is possible for the values lie in the interval $0 < \beta < 1$ and $-1 < sw < 1$ respectively. The curvature of the ZVC is obtained and noticed that when the curves bend to each other then connection is open and the body moves from one allowed side to other side however when the curve is not bended then curve goes outside and the body does not move one allowed side to other side.

We have obtained the particular solutions, which are the extreme values of Jacobi function. It is found that three collinear points for the values of $0 < \beta < 0.1$ are real whereas only one real point exists when $0.125 < \beta < 1$. We have determined the co-ordinates of two non-collinear points which depend on radiation pressure and the solar wind drag. With the help of PSS, it is observed that the stability region get expanded in presence of radiation pressure and solar wind drag and at the point $\xi = 0.025$ orbits are stable. Further, we estimated the LCE(λ) for the maximal time of evolution $0 \leq t \leq 10000$ and found that it is negative which shows that orbit of the infinitesimal

body is regular. Since it is difficult to obtained an exact expression of pseudo potential function in presence of term due to dissipative force, therefore further work is needed in this regard. This work may be applicable to study the motion of test particle in coupled restricted three body problem with drag forces.

We are thankful to IUCAA, Pune for partially financial support to visit library and to use computing facility. We are also thankful to Prof. Ishwar, B.R.A. Bihar University, Muzaffarpur (India) and Mr. Ram Kishor, ISM, Dhanbad (India) for their valuable suggestions during the preparation of the manuscript. We are grateful to anonymous referee for his constructive comment regarding improvement (Glasman-Deal 2010) of manuscript.

REFERENCES

- Benettin G, Galgani L, Giorgilli A, Strelcyn JM (1980) Lyapunov characteristic exponents for smooth dynamical systems and for Hamiltonian systems - A method for computing all of them. I - Theory. II - Numerical application. *Meccanica* 15:9–30
- Burns JA, Lamy PL, Soter S (1979) Radiation forces on small particles in the solar system. *Icarus*40:1–48, DOI 10.1016/0019-1035(79)90050-2
- Ceccaroni M, Biggs J (2012) Low-thrust propulsion in a coplanar circular restricted four body problem. *Celestial Mechanics and Dynamical Astronomy* 112:191–219, DOI 10.1007/s10569-011-9391-x
- Froeschle C (1984) The Lyapunov characteristic exponents - Applications to celestial mechanics. *Celestial Mechanics* 34:95–115, DOI 10.1007/BF01235793
- Glasman-Deal H (2010) Science Research Writing: A Guide for Non-Native Speakers of English. Imperial College Press, URL <http://books.google.co.in/books?id=nu9LZ1x818oC>
- Hadjidemetriou JD (1980) The restricted planetary 4-body problem. *Celestial Mechanics* 21:63–71, DOI 10.1007/BF01230248

- Huang SS (1968) A hypothetical four-body problem and its applications. *Vistas in Astronomy* 10:113–124, DOI 10.1016/0083-6656(68)90042-1
- Ishwar B, Kushvah BS (2006) Linear Stability of Triangular Equilibrium Points in the Generalized Photogravitational Restricted Three Body Problem with Poynting-Robertson Drag. *Journal of Dynamical Systems and Geometric Theories* 4:79–86, [arXiv:math/0602467](https://arxiv.org/abs/math/0602467)
- Kalvouridis TJ, Arribas M, Elipe A (2006) The Photo-Gravitational Restricted Four-Body Problem: An Exploration of Its Dynamical Properties. In: Solomos N (ed) *Recent Advances in Astronomy and Astrophysics*, American Institute of Physics Conference Series, vol 848, pp 637–646, DOI 10.1063/1.2348041
- Kushvah BS (2008) The effect of radiation pressure on the equilibrium points in the generalized photogravitational restricted three body problem. *Ap&SS*315:231–241, DOI 10.1007/s10509-008-9823-6, 0801.3369
- Liou JC, Zook HA, Jackson AA (1995) Radiation pressure, Poynting-Robertson drag, and solar wind drag in the restricted three-body problem. *Icarus*116:186–201, DOI 10.1006/icar.1995.1120
- Machuy AL, Prado AFBA, Stuchi TJ (2007) Numerical study of the time required for the gravitational capture in the bi-circular four-body problem. *Advances in Space Research* 40:118–124, DOI 10.1016/j.asr.2007.02.069
- Marčeta D (2012) Some aspects of circular restricted three-body problem from differential geometry point of view. In: Tsvetkov DM-STKKO M K, Mijačlović v (eds) *VII Bulgarian-Serbian Astronomical Conference (VII BSAC)*, *Astron. Soc. "Rudjer Bošković"* No 11, 2012, 247-251, pp 247–251
- Medvedev YD, Perov NI (2008) Restricted four-body problem. The case of a central configuration: Libration points and their stability. *Astronomy Letters* 34:357–365, DOI 10.1134/S1063773708050095
- Michalodimitrakis M (1981) The circular restricted four-body problem. *Ap&SS*75:289–305, DOI 10.1007/BF00648643
- Murray C, Dermott S (1999) *Solar System Dynamics*. Cambridge University Press, URL <http://books.google.co.in/books?id=NY9iQgAACAAJ>
- Murray CD (1994) Dynamical effects of drag in the circular restricted three-body problem. 1: Location and stability of the Lagrangian equilibrium points. *Icarus*112:465–484, DOI 10.1006/icar.1994.1198
- Oseledec V (1968) A multiplicative ergodic theorem, Lyapunov characteristic numbers for dynamical systems. *Transactions of Moscow Mathematics Society* 19:197–231
- Papadakis KE (2007) Asymptotic orbits in the restricted four-body problem. *Planet. Space Sci.*55:1368–1379, DOI 10.1016/j.pss.2007.02.005
- Poincaré H (1892) *Les methodes nouvelles de la mecanique celeste*
- Poynting JH (1903) Radiation in the solar system : its effect on temperature and its pressure on small bodies. *MNRAS*64:A1
- Ragos O, Zafiropoulos FA, Vrahatis MN (1995) A numerical study of the influence of the Poynting-Robertson effect on the equilibrium points of the photogravitational restricted three-body problem II. Out of plane case. *A&A*300:579
- Robertson HP (1937) Dynamical effects of radiation in the solar system. *MNRAS*97:423
- Rosaev A (2011) Capture in restricted four body problem. *ArXiv e-prints* 1111.3755
- Schuerman DW (1980) The restricted three-body problem including radiation pressure. *ApJ*238:337–342, DOI 10.1086/157989
- Skokos C (2010) The Lyapunov Characteristic Exponents and Their Computation. In: Souchay J, Dvorak R (eds) *Lecture Notes in Physics*, Berlin Springer Verlag, *Lecture Notes in Physics*, Berlin Springer Verlag, vol 790, pp 63–135, DOI 10.1007/978-3-642-04458-8\2, 0811.0882

Winter OC (2000) The stability evolution of a family of simply periodic lunar orbits. Planet. Space Sci.48:23–28, DOI 10.1016/S0032-0633(99)00082-3

Wolfram S (2003) The mathematica book. Wolfram Media, URL <http://books.google.co.in/books?id=dyK0hmFkNpAC>